

## Development of a High-current Microbeam System

著者	Matsuyama S., Ishii K., Suzuki S., Terakawa A., Fujiwara M., Koshio S., Toyama S., Ito S., Fujisawa M., Nagaya T.
journal or publication title	CYRIC annual report
volume	2014-2015
page range	37-41
year	2015
URL	<a href="http://hdl.handle.net/10097/00120743">http://hdl.handle.net/10097/00120743</a>

## IV. 1. Development of a High-current Microbeam System

*Matsuyama S., Ishii K., Suzuki S., Terakawa A., Fujiwara M., Koshio S., Toyama S., Ito S., Fujisawa M., and Nagaya T.*

*Department of Quantum Science and Energy Engineering, Tohoku University*

### 1. Introduction

Characterization of the spatial distribution of elements in a specimen is an important technique. A microbeam system was installed at a Dynamitron laboratory at Tohoku University in 2002 and has been used in several different fields<sup>1)</sup>. The microbeam system has been applied to simultaneous in-air/in-vacuum PIXE, RBS, SE, and STIM analyses, with applications in various fields<sup>2-6)</sup>. While this analysis system is applicable to simultaneous in-air/vacuum PIXE, RBS, and STIM analyses, as well as 3D  $\mu$ CT without changing the target chamber<sup>7)</sup>, changes are required in the equipment setup with these techniques, which is time-consuming, and a new high-energy-resolution  $\mu$ -PIXE system for chemical state mapping is planned. For this, a wavelength-dispersive X-ray (WDX) spectrometer with a high-energy resolution was developed. By combining the WDX and microbeam systems, the chemical state of elements can be mapped. Although the WDX system can be also adapted to the microbeam line without changing the target chamber, the WDX system is large, and precise adjustments are required. To meet these requirements, another microbeam line was recently developed in the Dynamitron laboratory dedicated to chemical state mapping, i.e., a von Hamos X-ray spectrometer with a charge-coupled device (CCD) camera. Although the sensitivity of the WDX system was higher than that of conventional crystal spectrometers in terms of detection efficiency, larger beam currents are required in the microbeam system. In this work, we developed a high-current microbeam system dedicated to the WDX- $\mu$ -PIXE system for chemical state mapping.

### 2. Design of the high-current microbeam system

A microbeam system was developed for the WDX- $\mu$ -PIXE system and designed so

that the spot size of the beam was  $1 \times 1 \mu\text{m}^2$  with a beam current of several hundred pA. This new microbeam system is termed MB-II to distinguish it from the existing microbeam system (i.e., MB-I, which was developed for biological applications with the aim of achieving a submicron beam size<sup>8-11</sup>). The energy stability of the accelerator was significantly improved to  $<10^{-4}$ , which is sufficient for submicron beam formation in the doublet system without requiring an analysis system<sup>8,9,10</sup>. MB-II was installed in the  $-15^\circ$  beam line. This arrangement allows for a total length of the microbeam line of 7 m. The lens system of MB-II was a quadrupole doublet, and the spherical and chromatic aberration coefficients of the doublet system are smaller than those of the triplet system<sup>8,9</sup>). The beam properties were calculated using TRANSPORT<sup>12</sup>) and the ray-tracing software package WinTRAX<sup>13</sup>). The working distance was 24 cm, and the separation from the object slit to the quadrupole doublet lens was 6.04 m. The demagnification factors were 38 in the horizontal plane and 9.5 in the vertical plane. The spot size of the beam was  $1 \times 1 \mu\text{m}^2$  when the beam divergence was limited to 0.2 mrad and the object size was  $40 \times 10 \mu\text{m}^2$ . Figure 2 shows a diagram of the layout of MB-II; the system was composed of a quadrupole doublet lens, a micro-slit (MS), and a divergence-defining slit (DS). The total length of the line was approximately 7 m. The MS defines the object size, and the DS defines the beam divergence into the quadrupole doublet, which was located 5.22 m downstream of the MS. In MB-I, a baffle slit (BS) was used to reduce the scattered beam. These components were mounted on a heavy rigid support to provide vibration isolation, which was placed on three concrete blocks with dimensions of  $70 \times 70 \times 70 \text{ cm}^3$ .

### 3. Performance

#### 3.1. Beam brightness

The beam brightness is of primary importance to increase the current of the focused beam. The beam brightness was characterized by measuring the target current in the microbeam with the MS fixed, while varying the DS. The MS widths were  $40 \times 10 \mu\text{m}^2$ , which corresponds to a beam spot size of  $1 \times 1 \mu\text{m}^2$ . The largest beam brightness of MB-I was  $2.3 \text{ pA} \cdot \mu\text{m}^{-2} \cdot \text{mrad}^{-2} \cdot \text{MeV}^{-1}$  with a half-divergence of 0.07 mrad. Since the beam line to MB-II is short compared with that of MB-I, the beam brightness at MB-II will be larger than that at MB-I, and the beam transport conditions for MB-II will differ from those of MB-I. The terminal equipment of the Dynamitron accelerator comprises a duoplasmatron ion source along with an extractor, an Einzel lens, an ExB filter, and a gap lens<sup>14</sup>). The

extraction voltage and gap lens voltage significantly affects the beam brightness, which determines the lens effects. These parameter was confirmed by both calculations using OPTIC-III (National Electrostatic Corporation, NEC) and by experiments<sup>8,11,14</sup>). A large beam brightness of  $2.4 \text{ pA} \cdot \mu\text{m}^{-2} \cdot \text{mrad}^{-2} \cdot \text{MeV}^{-1}$  was achieved with a half-divergence of 0.1 mrad. The beam brightness of MB-I was decreased significantly for larger divergences, which means the beam intensity was stronger in the central region. The beam brightness at MB-II, however, did not diminish as the beam divergence increased. This difference results from the different beam loss of the beam line components between the accelerator and MB-I. Due to the small spherical and chromatic aberration coefficients, the beam divergence into the quadrupole lens was 0.2 mrad in MB-II. A beam current of more than 300 pA was obtained for a beam spot size of  $1 \times 1 \mu\text{m}^2$ , which is larger than that of MB-I.

### 3.2. Beam spot size

The spot size of the beam was characterized via beam scanning across fine mesh samples (Ni meshes, with 2000 lines per inch) by measuring X-rays. The horizontal and vertical line profiles shown in Figure 3. The horizontal and vertical line profiles were fitted using symmetric double Gaussian convolution to obtain the spot sizes. The line profiles were well reproduced using symmetric double Gaussian convolution, which implies that the beam profile can be assumed to be Gaussian. A spot size of  $1 \times 1.5 \mu\text{m}^2$  was obtained with an MS opening of  $40 \times 10 \mu\text{m}^2$ .

## 4. Conclusions

We developed an MB-II high-current microbeam system dedicated for chemical state mapping, which was composed of two slits and a quadrupole doublet lens mounted on a heavy rigid support. The microbeam system was not equipped with a high-resolution energy analysis system and was connected to a switching magnet. The largest beam brightness was  $2.4 \text{ pA} \cdot \mu\text{m}^{-2} \cdot \text{mrad}^{-2} \cdot \text{MeV}^{-1}$  at a half-divergence of 0.1 mrad. A beam current greater than 300 pA was obtained for an object size of  $40 \times 10 \text{ mm}^2$  with a half divergence of 0.2 mrad. The calculated spot size of the beam was  $1 \times 1 \mu\text{m}^2$ , and the measured spot size was  $1 \times 1.5 \mu\text{m}^2$ . The WDX- $\mu$ -PIXE system is currently operational at the microbeam system.

## Acknowledgments

This study was partly supported by a Grant-in-Aid for Challenging Exploratory Research Grant No. 26630477 from the Japan Society for the Promotion of Science (JSPS).

## References

1. Matsuyama S, Ishii K, Yamazaki H, et al., *Nucl Instrum Meth B* **210** (2003) 59.
2. Matsuyama S, Ishii K, Yamazaki H, et al., *Int J PIXE* **18** (2008) 199.
3. Matsuyama S, Ishii K, Fujiwara M, et al., *Int J PIXE* **19** (2009) 61.
4. Matsuyama S, Ishii K, Fujiwara M, et al., *Int J PIXE* **21** (2011) 87.
5. Ishii K, Matsuyama S, Yamazaki H, et al., *Nucl Instrum Meth B* **249** (2006) 726.
6. Ishii K., Matsuyama S., Y. Y. Watanabe, et al., *Nucl Instrum Meth A* **571** (2007) 64.
7. Matsuyama S, Ishii K, Yamazaki H, et al., *Nucl Instrum Meth B* **260** (2007) 55.
8. Matsuyama S, Ishii K, Tsuboi S, et al., *Int J PIXE* **21** (2011) 87.
9. Matsuyama S, Ishii K, Watanabe K, et al., *Nucl Instrum Meth B* **318** (2014) 32.
10. Matsuyama S., Fujisawa M, Nagaya T, et al., *Int J PIXE* **23** (2013) 69.
11. Matsuyama S, Watanabe K, Ishii K, to be published in *Int J PIXE*.
12. Brown KL, SLAC-91 (1977).
13. Grime GW, *Nucl Instrum Meth B* **306** (2013) 2060.
14. Matsuyama S, Ishii K, Fujisawa M, et al., *Nucl Instrum Meth B* **267** (2009) 2060.

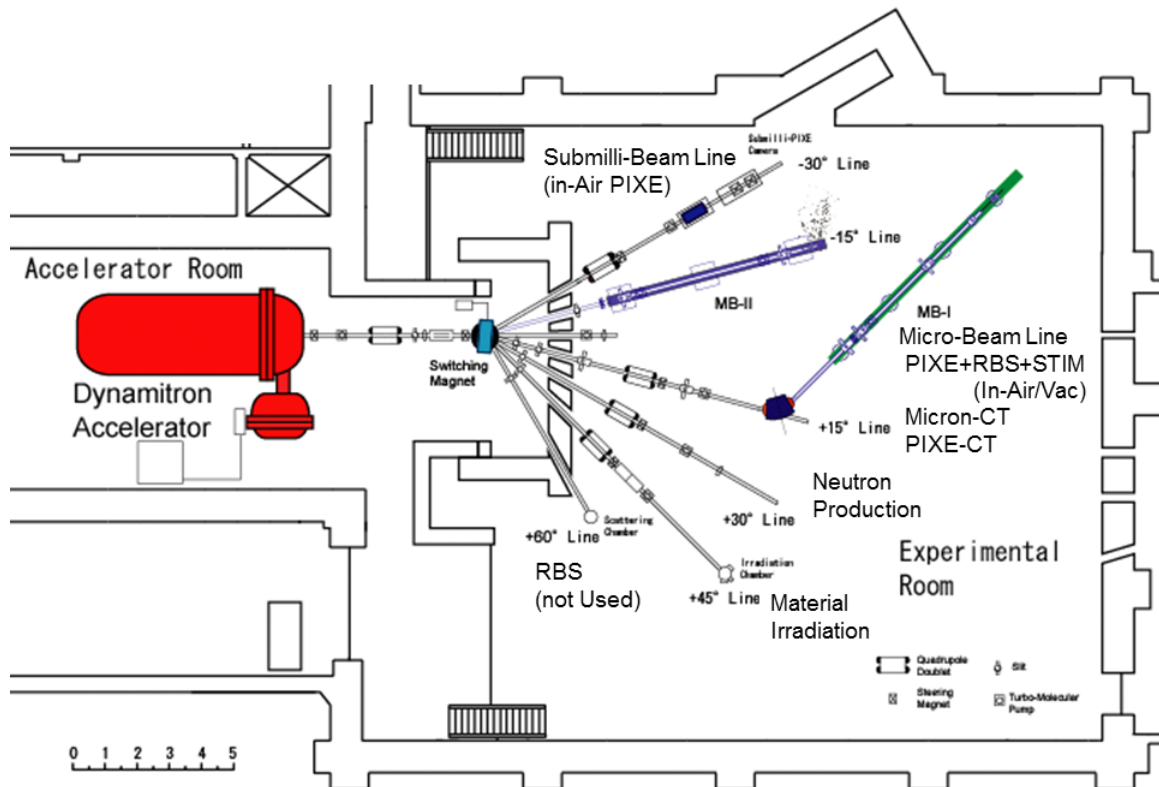


Figure 1. The layout of the Dynamitron laboratory.

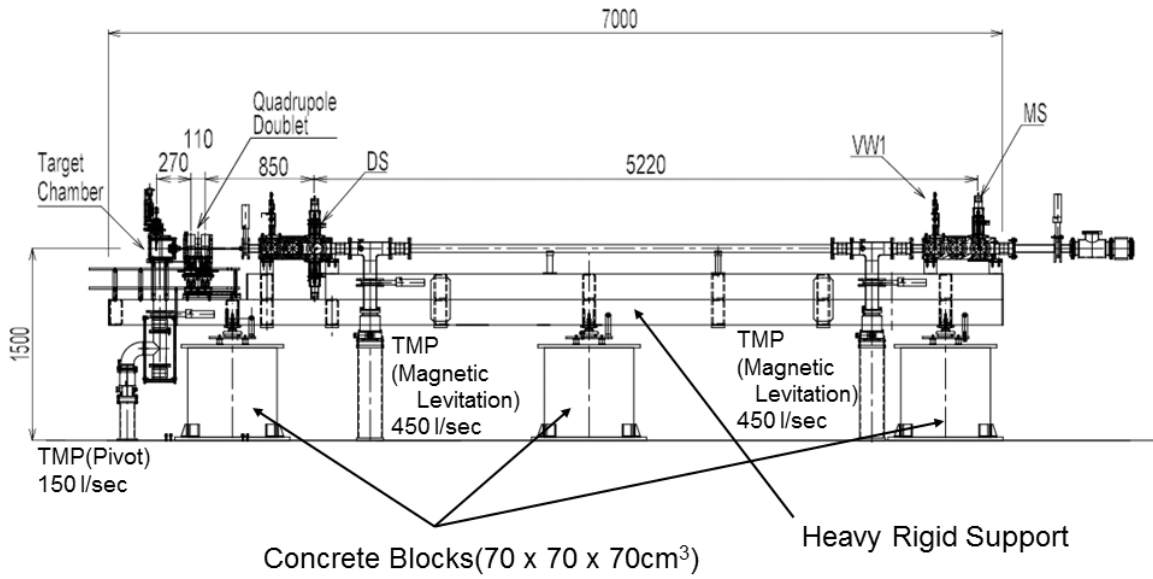


Figure 2. Scale drawing of the microbeam system.

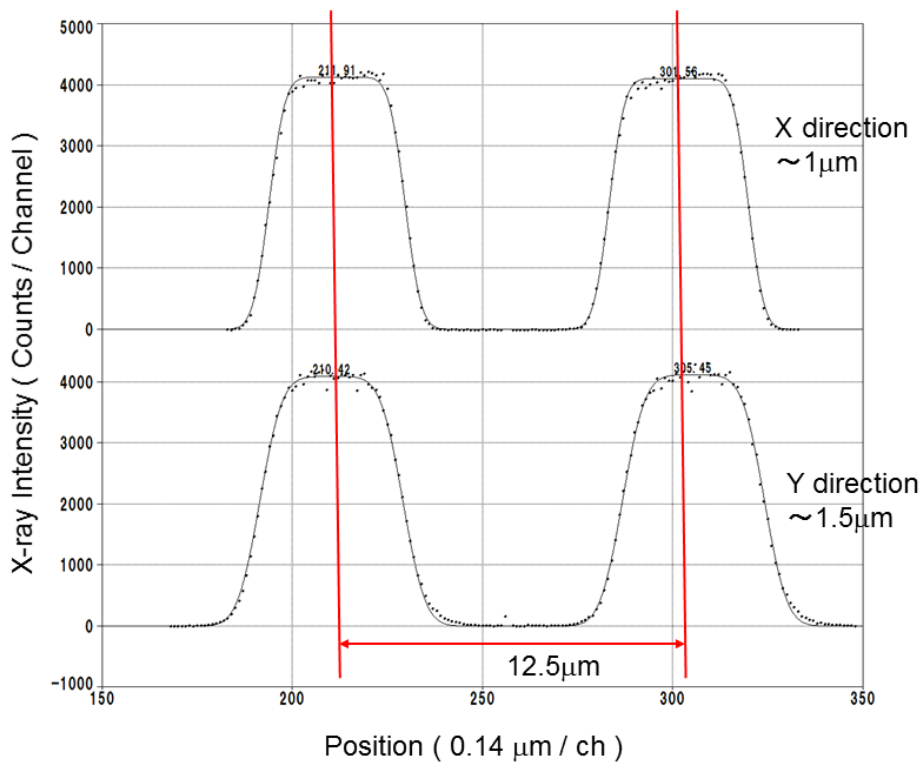


Figure 3. The horizontal and vertical X-ray line profiles of a fine Ni mesh (2000 lines/inch).